

# Hall effect and electronic structure of $\text{La}_{2-x}\text{Sr}_x\text{CuO}_4$

J. Ruvalds and A. Virosztek\*

*Physics Department, University of Virginia, Charlottesville, Virginia 22901*

(Received 28 February 1990)

The unusual Hall coefficient  $R_H$  observed in  $\text{La}_{2-x}\text{Sr}_x\text{CuO}_4$  single crystals is explained in terms of strong electron-electron scattering in a nearly half-filled  $\text{Cu } d_{x^2-y^2}$  band  $E_1$ , together with a small number of holes in another band. Including multiple-scattering terms beyond the Born approximation yields an electron mobility that decreases dramatically as the Sr content is lowered toward  $x \approx 0.06$ . There, a metal-insulator transition is predicted by our analysis for an on-site Coulomb coupling  $U$  of intermediate strength. Hence the minority-hole carriers yield a net positive  $R_H$  for  $x < 0.4$  by virtue of their higher mobility. Surprisingly, despite changes in  $R_H$  by orders of magnitude, the calculated plasma frequency remains nearly constant with  $\omega_p \approx 0.8$  eV over the metallic  $x$  range, in agreement with reflectivity data.

## I. INTRODUCTION

Following the discovery<sup>1</sup> of high-temperature superconductivity, studies of the normal-state properties of  $\text{La}_{2-x}\text{Sr}_x\text{CuO}_4$  have provided vital clues to the electronic structure. Theoretical attempts to identify mechanisms for the superconductivity rely on the nature of the charge carriers and are particularly constrained by the number of electrons or holes in the superconducting phases.

The Hall coefficient  $R_H$  provides a classic determination of the sign and density of the charge carriers. Estimates of the plasma frequency  $\omega_p$  provide additional constraints on the carrier density. Thus it is particularly puzzling that the Hall data<sup>2,3</sup> on  $\text{La}_{2-x}\text{Sr}_x\text{CuO}_4$  shows a drop in  $R_H$  by two orders of magnitude as the Sr content is increased from  $x=0.1$  to  $x=0.3$ , whereas the reflectivity data<sup>3</sup> on the single-crystal samples yield a plasmon energy which is essentially constant over the same range.

Other anomalous features of the transport properties measured<sup>3</sup> on single-crystal films include (a) at  $x=0.04$ ,  $R_H \approx 1/x$  and is essentially independent of temperature; (b) for  $0.1 \leq x \leq 0.36$  there is a considerable temperature variation to  $R_H$  and  $R_H$  is far below the  $1/x$  curve at higher  $x$ ; (c) the dc resistivity  $\rho$  decreases dramatically as the Sr content is increased, with an order of magnitude drop in  $\rho$  as  $x$  increases from 0.04 to 0.10; (d) at higher concentrations, say  $0.1 < x < 0.4$ , the residual resistivity is metallic with  $\rho(T=0) \approx 100 \mu\Omega \text{ cm}$ , and the temperature variation of  $\rho(T)$  departs somewhat from the linear dependence characteristics of many cuprate samples.

The variation of the Hall coefficient as a function of Sr content is shown at two temperature values in Fig. 1.<sup>3</sup> At small  $x$ ,  $R_H$  is large and positive, in contrast to the conventional expectation for the doping of a nearly half-filled band with electrons having normal mobility. On the other hand, the large  $x$  region shows a large departure from the  $R_H = 1/x$  curve which would be expected from the straightforward doping of a single band of holes in the effective-mass approximation. Our goal is to un-

derstand the  $R_H$  variation over the entire  $x$  range and yet retain consistency with the observed plasmon energy which does not change over the same range.

The temperature variation of the Hall coefficient leads naturally to the consideration of two energy bands whose

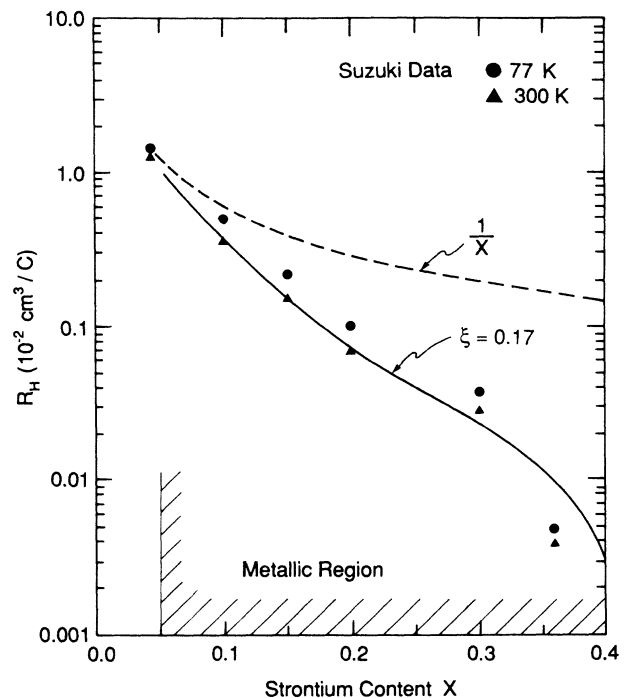


FIG. 1. Hall coefficient  $R_H$  is shown as a function of Sr content. Data for  $T=77$  and 300 K is from single-crystal thin films (Suzuki, Ref. 3). The dashed line shows the  $1/x$  behavior expected for a single band in the effective-mass approximation. The solid curve follows from our two-band analysis with  $\xi=0.17$ ,  $U \approx 0.7$  eV, and the bands with the Fermi energy placement described in the text and shown in Fig. 2.

individual mobilities may be different. We select two bands in the tight-binding approximation, with the simple dispersion

$$E_l = 2t_l [\cos(ak_x) + \cos(ak_y)] , \quad (1)$$

for the majority carriers presumed to originate from the Cu  $d_{x^2-y^2}$  orbital. The bandwidth of  $8t_l = 4.0$  eV is chosen in correspondence to augmented plane wave (APW) computational results for  $\text{La}_2\text{CuO}_4$ .<sup>4,5</sup> The second narrower band is slightly below the half-filling energy  $E_l = 0$ , and is described by

$$E_h = \delta + 2t_h [\cos(ak_x) + \cos(ak_y) - 2] , \quad (2)$$

where  $\delta = -0.02$  eV and  $t_h = 0.1$  eV yields a remarkably good description of the Hall data as we shall see below.

These energy bands along with the placement of the Fermi energy  $E_F$  at two selected Sr concentrations are shown in Fig. 2. The position of the second orbital relative to the Fermi energy is a key feature of our analysis. Doping  $\text{La}_2\text{CuO}_4$  with Sr lowers  $E_F$ , and our proposal that  $E_F$  intersects the narrower  $E_h$  band is an extrapolation of the general features of the band structure results.<sup>4,5</sup> However, our simple model is chosen to allow an analytic calculation of the many body scattering contribution to the electron mobility, and therefore will not reproduce the detailed structures of the bands obtained from computer calculations.

Our derivation of the Hall coefficient for the above tight-binding electronic structure is presented in Sec. II. The electron mobility is found to be a highly sensitive

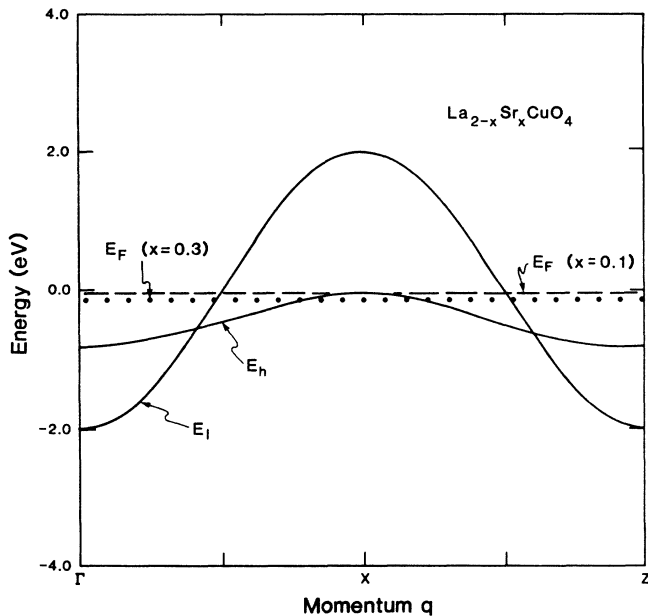


FIG. 2. Electronic structure of  $\text{La}_{2-x}\text{Sr}_x\text{CuO}_4$  with the Fermi energy  $E_F$  relative to the tight-binding bands  $E_l$  (originating from the Cu  $d_{x^2-y^2}$  orbital) and the narrow  $E_h$  band which may correspond to the Cu  $d_{z^2}$  orbital. Both Cu levels are hybridized with the oxygen  $p$  states.

function of the Sr content as a result of strong electron-electron coupling, and these features are in Sec. III. The plasma frequency computations are in Sec. IV, and the conclusions of our study are in Sec. V.

## II. HALL EFFECT

The Hall coefficient is derived from the standard formulas using a zero temperature approximation for the Fermi function to obtain the conductivity

$$\sigma_{xx} = \sigma_{yy} = \frac{e^2}{2\pi^2} \tau(E_F) \int d^2k \delta(E_k - E_F) v_x^2(\mathbf{k}) , \quad (3)$$

where the relaxation time  $\tau$  is presumed independent of momentum. Performing the integration over the  $\delta$  function  $\delta(E_k - E_F)$  yields a one-dimensional integral which may be evaluated exactly for our model using  $\mathbf{v} = \nabla_{\mathbf{k}} E(\mathbf{k})$  to obtain

$$\sigma_{xx} = \frac{4e^2\tau}{\pi^2} t_j B_j(E_F) , \quad (4)$$

where the function  $B_j$  is

$$B_j = \int_0^{x_0} dx [1 - (-\varepsilon/2t_j - \cos x)^2]^{1/2} , \quad (5)$$

with  $x = ak_x/\pi$  and the cutoff  $x_0 = ak_{Fx}/\pi$  is the dimensionless Fermi wave vector. Expressing the cutoff in terms of the Fermi energy for each tight-binding band  $E_j$  yields the analytic result in terms of elliptic functions  $E(y)$  and  $K(y)$  as

$$B_j = 2E(y) + 2\xi[2K(y) - E(y)] , \quad (6)$$

where  $i=l$  refers to the nearly half-filled  $E_l$  band and  $i=h$  denotes the hole contribution of the  $E_h$  band. The variables are  $y = (1 + \xi)/(1 - \xi)$ , with  $\xi = \varepsilon/4t_i$ , denoting the energy  $\varepsilon$  measured from the middle of a given  $E_i$  band in Eqs. (1) and (2).

Similarly, we obtain

$$\begin{aligned} \sigma_{yx} &= -\sigma_{xy} \\ &= \frac{H|e|^3\tau^2}{2\pi^2} \int d^2k \delta(E_k - E_F) v_x^2(\mathbf{k}) \left[ \frac{\partial}{\partial k_y} v_y(\mathbf{k}) \right] , \end{aligned} \quad (7)$$

which reduces to

$$\sigma_{yx} = 8H|e|^3\tau^2 \left[ \frac{at_j}{\pi} \right]^2 A_j(E_F) , \quad (8)$$

where

$$A_j = \int_0^{x_0} dx \cos(x) [1 - (-\varepsilon/2t_j - \cos x)^2]^{1/2} . \quad (9)$$

In terms of the elliptic functions  $E(y)$  and  $K(y)$ ,

$$A_j = -2\xi[2K(y) - (1 - \xi)E(y)] , \quad (10)$$

where  $H$  is the applied magnetic field perpendicular to the  $xy$  plane, the Hall coefficient measured along the Cu-O planes is

$$R_H = \frac{\sigma_{yx}}{H\sigma_{xx}\sigma_{yy}} = \frac{(\pi a)^2}{2e} \frac{A_h + \alpha^2 A_l}{(B_h + \alpha B_l)^2} , \quad (11)$$

where  $\alpha = \tau_l t_l / \tau_h t_h$  is the ratio of relaxation times  $\tau_j$  and bandwidths  $t_j$  for the individual bands.

Over the Sr content range of interest here, it is a good approximation to use the expansions for the nearly half-filled  $E_l$  band

$$A_l \simeq -2\xi \left[ \ln \frac{4}{|\xi|} - 1 \right] + O(\xi^2), \quad (12)$$

and the small filling of the narrower  $E_h$  band allows

$$A_h \simeq -2\pi\delta \left[ 1 - \frac{1}{2}\delta - \frac{1}{4}\delta^2 + O(\delta^3) \right], \quad (13)$$

where  $\delta = (1 - \xi)/2$ . Similarly the  $B_j$  function has the useful expansions for the nearly half-filled  $E_l$  band,

$$B_l \simeq 2 - \xi^2 \left[ 0.5 + \ln \frac{4}{|\xi|} \right], \quad (14)$$

and the corresponding hole band contribution

$$B_h \simeq 2\pi\delta \left[ 1 - \frac{1}{2}\delta - \frac{1}{4}\delta^2 + O(\delta^3) \right]. \quad (15)$$

A key feature of the analysis is the choice of relaxation processes which determine the mobility ratio  $\alpha$ . Choosing a constant scattering rate  $\tau_h = \tau_l$  in our model yields an inadequate negative Hall coefficient whose value is an order of magnitude smaller than the observed positive  $R_H$  values at low  $x$  shown in Fig. 1. A more refined band structure topology analysis<sup>6</sup> with a constant relaxation rate approximation also yields values of  $R_H$  smaller than the observations, although the topology corrections yield a small  $R_H$  which is positive at low  $x$ , but then becomes negative for  $x \geq 0.25$ . Thus the band-theory analysis anticipated a sign change in  $R_H$  at higher doping levels, and the trend of the measured Hall effect in Fig. 1 suggests that possibility for  $x \sim 0.4$ . A major success of the earlier band-theory analysis<sup>6</sup> is the prediction of a nearly constant plasma frequency over a wide  $x$  range in agreement with the reflectivity data. By contrast, the standard form of the strong coupling Mott-Hubbard model based on the slight doping of holes in a single band would presumably indicate  $R_H \sim 1/x$  and  $\omega_p \sim x^{1/2}$ .

On the other hand, band theories have been criticized because their single-particle basis leads to a metallic state even at  $x=0$ , whereas the host  $\text{La}_2\text{CuO}_4$  compound is an insulator. A possible resolution of this dilemma is the instability of a half-filled two-dimensional (2D) tight-binding band of itinerant electrons toward the formation of an insulating spin-density wave (SDW) state.<sup>7,8</sup> Within the constant relaxation time approximation, the latter viewpoint would suggest a negative Hall coefficient for the metallic  $\text{La}_{2-x}\text{Sr}_x\text{CuO}_4$  alloys, however, and this discrepancy provided the primary motivation for our analysis.

### III. ELECTRON MOBILITY

The new element in our analysis is the calculation of multiple-scattering electron-electron processes which have a remarkable influence on the mobility of electrons in a nearly half-filled tight-binding band such as the  $E_l$

structure shown in Fig. 2. In two dimensions the  $E_l$  band exhibits a  $\ln \epsilon$  singularity in the electron density of states, where  $\epsilon=0$  refers to a Fermi energy in the middle of the band. Within the Born approximation, we would find simply  $\tau_l^{-1} \propto \ln(\epsilon)$  and therefore a vanishing mobility for electrons with  $\epsilon=0$ . Of course this divergence indicates the need for higher order scattering corrections even in the metallic regions of large Sr content  $x$  which corresponds to  $\epsilon \neq 0$ . Physically the point is that the electron-electron scattering may diminish the electron mobility at small  $x$  and therefore allow the smaller number of holes in the  $E_h$  band to dominate the Hall coefficient. Hence increasing  $x$  corresponds to lowering  $E_F$  away from the  $\epsilon \simeq 0$  case, and raising the electron mobility.

The electron scattering rate is calculated by including multiple-scattering events in the ladder diagram series, which yields

$$\frac{1}{\tau_l} \simeq \frac{2U^2}{N} \sum_{\mathbf{q}} \frac{1}{\sinh \left[ \frac{\eta}{T} \right]} \frac{\chi''(\mathbf{q}, \eta)}{[1 - U\chi'(\mathbf{q}, \eta)]^2 + [U\chi''(\mathbf{q}, \eta)]^2}, \quad (16)$$

where  $\eta = E_l(\mathbf{k} - \mathbf{q}) - E_F$ , and  $U$  is the on-site Coulomb repulsion between electrons of opposite spins. We consider three cases to distinguish the importance of Fermi surface nesting which is inherent in the nearly half-filled tight-binding band  $E_l$ . For contrast, we consider (Sec. III A) conventional Fermi-liquid behavior, (Sec. III B), the nested 2D band in the Born approximation, and (Sec. III C) the multiple-scattering features which may diminish the electron mobility by orders of magnitude, and induce a severe concentration dependence in  $\tau_l(x)$ .

#### A. Fermi-liquid behavior

The inadequacy of a conventional Fermi liquid (FL) for  $\text{La}_{2-x}\text{Sr}_x\text{CuO}_4$  is characterized by a low electric resistivity  $\rho_{\text{FL}} \propto \tau_{l,\text{FL}}^{-1} \propto T^2$  in contrast to the data<sup>3</sup> which show a nearly linear  $T$  variation. Furthermore, the relatively longer lifetime  $\tau_{l,\text{FL}}$  would suggest an overall negative Hall coefficient in the case where electrons outnumber holes. In two dimensions the density of states in the effective-mass approximation  $N_{\text{FL}}(E_F)$  is constant, and thus changes in the Sr doping should not yield much change in the electron-electron scattering contribution to  $\tau_{l,\text{FL}}$ .

These features follow from Eq. (16) in a simple way because the Born approximation should be adequate. Thus the conventional result is

$$\frac{1}{\tau_{l,\text{FL}}} \simeq \frac{2U^2}{N} \sum_{\mathbf{q}} \frac{1}{\sinh(\eta/T)} \chi''(\mathbf{q}, \eta). \quad (17)$$

Using the momentum average for the susceptibility  $\langle \chi''(\mathbf{q}, \eta) \rangle_{\mathbf{q}} \simeq \pi \eta N_{\text{FL}}^2(E_F)$

$$\frac{1}{\tau_{l,\text{FL}}} \simeq 2\pi U^2 N_{\text{FL}}^2 \frac{1}{N} \sum_{\mathbf{q}} \frac{\eta}{\sinh(\eta/T)}. \quad (18)$$

Performing the integration, we obtain the standard result

$$\frac{1}{\tau_{l,FL}} \simeq U^2 \pi^3 N_{FL}^3(E_F) T^2 \simeq \frac{\pi^3 U^2 T^2}{W^3}, \quad (19)$$

where  $N_{FL}(E_F) \sim 1/W$  in the 2D band of width  $W$ . Clearly  $\tau_{l,FL}^{-1}$  should be small for  $W \sim 4$  eV, and the insensitivity of  $\tau_{l,FL}$  to doping is evident from Eq. (19).

Impurity scattering provides an additional constraint on the  $\tau_l$  lifetime, but the ordinary expectation would be that increasing Sr content in the *metallic* state  $x > 0.1$  should raise the resistivity. By contrast, the data<sup>3</sup> exhibit a clearcut systematic decrease in  $\rho$  ( $T > T_c$ ) at higher  $x$ . Thus we were led to examine structure in the density of states which is likely to occur in a 2D tight-binding electronic structure.

### B. Tight-binding Born approximation

The dominant contributions to the electron-electron scattering on a 2D square lattice involve the nesting wave vector  $\mathbf{Q} \simeq (\pm\pi/a, \pm\pi/a)$ , where the real and imaginary parts of the susceptibility  $\chi = \chi' + i\chi''$  diverge as  $\chi'(\mathbf{Q}, \omega) \sim \ln^2|\epsilon|$  and  $\chi''(\mathbf{Q}, \omega) \sim \ln|\epsilon|$ , respectively. Slight doping moves the Fermi energy away from the  $\epsilon=0$  logarithmic divergence, and the resulting analytic structure in  $\chi''(\mathbf{Q}, \omega)$  leads to a linear  $T$  variation of the resistivity.<sup>9</sup>

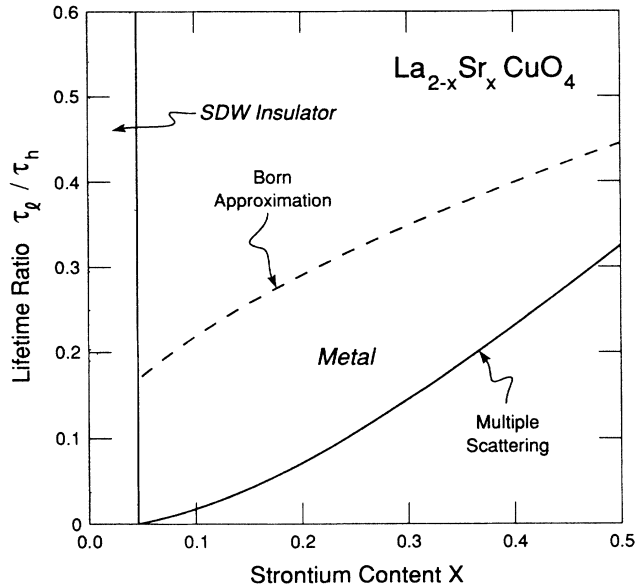


FIG. 3. Ratio of lifetimes  $\tau_l/\tau_h$  (which is proportional to the electron mobility) is shown as a function of Sr doping  $x$ . Within the Born approximation of the dashed curve, the electron-electron scattering yields an enhanced electron lifetime  $\tau_l$  with the addition of Sr because the Fermi energy is shifted to a region of lower density of states. Multiple scattering strongly suppresses the electron mobility at low  $x$  as shown by the solid curve for intermediate Coulomb coupling  $U=0.7$  eV. The corresponding metal-insulator transition to an SDW state is expected at  $x \approx 0.06$  where the electron mobility vanishes.

The Born approximation neglects the higher order corrections beyond  $U^2$  which come from the denominator in Eq. (16). Presuming further that the scattering is dominated by the momentum region  $\mathbf{q} \simeq \mathbf{Q}$ , we make the replacement

$$\chi''(\mathbf{q}, \eta) \simeq \chi''(\mathbf{Q}, \eta) = \frac{\pi\eta}{8T} N_l(E_F), \quad (20)$$

where the  $E_l$  band density of states is

$$N_l(E_F) = \frac{1}{2\pi^2 t_l} \ln \left| \frac{16t_l}{E_F} \right|. \quad (21)$$

Then the  $\mathbf{q}$  integration in Eq. (16) yields the Born approximation result

$$\frac{1}{\tau_{l,Born}} \simeq \frac{U^2 T}{32\pi t_l^2} \ln^2 \left| \frac{16t_l}{E_F} \right|. \quad (22)$$

The divergence at half-filling (as  $E_F \rightarrow 0$ ) is evident, but it is confined to a narrow sliver of the energy region. The variation of  $\tau_{l,Born}$  with Sr content is shown in Fig. 3. Although there is an apparent smooth upturn in  $\tau_{l,Born}$  (and the electron mobility) as Sr doping increases, the variation nevertheless yields an inadequate Hall coefficient  $R_H(x)$ .

A more fundamental objection to the Born approximation is the known<sup>7,8</sup> SDW instability of the half-filled band which implies a metal-insulator transition whenever  $1 - U\chi'(\mathbf{Q}, 0) = 0$  at some critical concentration  $x$ . The ladder (RPA) series of diagrams that dominate the phase instability enter in Eq. (16), and yield a surprising suppression of the electron mobility as we show below.

### C. Multiple scattering

Analytic results for the  $E_l$  band mobility are obtained by the approximation  $\chi'(\mathbf{Q}, \eta) \simeq \chi'(\mathbf{Q}, 0)$  and neglecting  $\chi''$  in the denominator in Eq. (16) which yields the final result

$$\frac{1}{\tau_{l,L}} \simeq \frac{\pi^3}{8} U^2 N_l^2(E_F) T \frac{1}{[1 - U\chi'(\mathbf{Q}, 0)]^2}, \quad (23)$$

where

$$\chi'(\mathbf{Q}, 0) \simeq \frac{1}{(2\pi)^2 t_l} \ln^2 \left| \frac{16t_l}{E_F} \right| \quad (24)$$

also becomes divergent at half-filling, i.e.,  $E_F = 0$ .

The resulting strong energy dependence of  $\tau_l$  enters in the Hall effect via the parameter  $\alpha$  in Eq. (11). We consider  $\tau_h$  for the heavy band to be independent of energy, and therefore independent of the Sr content. The remarkable sensitivity of the electron mobility to the Sr doping is shown for the calculated relaxation rate ratio  $\tau_l/\tau_h$  in Fig. 3, where Eq. (24) yields the primary  $x$  variation and a constant ratio of scattering matrix elements  $\xi^{-1} \propto U\tau_h$  is used. The Born approximation result is shown by the dashed curve for  $\xi=0.17$  and on-site Coulomb interaction of intermediate strength  $U=0.7$  eV

in comparison to the bandwidth  $8t_l \approx 4.0$  eV. The higher order ladder graph corrections in Eq. (23) yield a much sharper drop in the electron relaxation time  $\tau_l$  as shown by the solid curve in Fig. 3. For these chosen model parameters there is an instability at  $x=0.06$  corresponding to a vanishing energy denominator in Eq. (23) and the associated phase transition from the metallic state ( $x \geq 0.06$ ) to an insulating phase with a spin-density wave (SDW). As the critical concentration  $x_c \approx 0.06$  is approached from above, higher order vertex corrections become progressively more important.<sup>10</sup> The Hall coefficient for our model follows from Eq. (11) with the calculated lifetime ratio providing a good fit to the measured  $R_H(x)$  over the entire  $x$  range shown in Fig. 1 by the solid curve. The agreement over the entire  $x$  range is quite reasonable considering that the shift in the Fermi energy  $E_F$  caused by the Sr content is treated in a very simple band model. The deviations at higher  $x$  values, e.g.,  $x=0.3$  and  $0.36$  may in fact indicate corrections to the narrow  $E_h$  band dispersion or to its placement relative to  $E_F$ . The present calculation suggests a change in sign of  $R_H$  for  $x \geq 0.46$ .

Negative  $R_H$  values have been reported in *polycrystalline* samples for  $x \geq 0.28$  in contrast to the single-crystal film data in Fig. 1. The discrepancy may be due to the fact that the Hall coefficient perpendicular to the Cu-O planes is negative even though the in-plane  $R_H$  is positive. Thus the analysis of the ceramic data requires an averaging process that is beyond our reach. A few data points on single-crystal samples<sup>11</sup> at  $x=0.34$  are in accord with the film data,<sup>3</sup> even though there is some variation between individual samples.

At the lowest Sr concentrations the divergence in the scattering rate at  $x \approx 0.06$  may indicate an instability related to the metal-insulator transition. For  $x=0.04$  and lower values, an energy gap is expected to occur in the  $E_l$  band whereas the Fermi energy is just near the top of the secondary  $E_h$  band. This situation would account for the much larger resistivity of the  $x=0.04$  sample, and the lack of a temperature variation to  $R_H$  in this case because only a few holes in the  $E_h$  band carry current. Also the temperature variation of the resistivity  $\rho(T)$  at  $x=0.04$  is similar to the variable range hopping form<sup>3</sup> in sharp contrast to the metallic behavior of  $\rho(T)$  for  $x \geq 0.06$ . These subsidiary observations impose additional constraints on our choice for the placement of the  $E_h$  band relative to the Fermi energy (i.e., the  $\delta$  parameter). Small changes in  $\delta$  would modify the calculated  $R_H$  as well as the resistivity  $\rho(T)$  at small  $x$  values near  $x \approx 0.04$ , and it may be possible to probe such changes externally by the application of uniaxial pressure to single crystals. This prospect may be relevant to the established sensitivity of the superconducting transition temperature to applied pressure<sup>12</sup> in ceramic examples. In the metallic samples with  $x \approx 0.1-0.36$ , the temperature variation of  $R_H$  can be attributed to differences in the relaxation times  $\tau_l$  and  $\tau_h$  for the two bands. The observed systematic decrease in  $R_H$  as  $T$  is increased from 77 to 300 K (shown in Fig. 1) may indicate a stronger increase in the narrow band scattering rate  $\tau_h^{-1}$  with temperature, by comparison to

the  $E_l$  band.

Normal-state resistivity  $\rho(T)$  data<sup>3</sup> show a significant *reduction* in resistivity with the addition of Sr. Hence it would appear that impurity scattering is weaker than electron-electron and electron-phonon processes. Our analysis suggests that the conductivity contributions of the two bands are comparable in magnitude for the two bands since the mobility of the nearly half-filled  $E_l$  band is limited by strong electron-electron scattering at small Sr content where the number of carriers in the  $E_h$  band is small. At larger values, of  $x \sim 0.3$  for example, the wider band  $E_l$  yields a substantial conductivity which may account for the evident decrease in  $\rho(T)$  as the increased Sr content shifts the Fermi energy away from half-filling.

The temperature variation of  $\rho(T)$  in earlier work<sup>9</sup> has been attributed to electron-electron scattering in a 2D nearly half-filled band. Their prediction of a linear  $T$  variation to  $\rho(T)$  with a crossover to a more conventional  $T^2$  dependence at different alloy compositions appears to be compatible with the latest single-crystal film data.<sup>3</sup>

Another interesting study<sup>13</sup> in the semiconducting phase of  $\text{La}_2\text{CuO}_{4+\delta}$  shows a Hall coefficient quite similar to examples of doped semiconductors, where the strong temperature variations of the conductivity and  $R_H$  are quite different from the metallic phases of the high Sr content alloys analyzed here.

#### IV. PLASMA FREQUENCY

Plasmon oscillations provide an independent probe of the electron or hole density, and hence it is remarkable that the measured reflectivity<sup>3,14</sup> on single-crystal films of  $\text{La}_{2-x}\text{Sr}_x\text{CuO}_4$  yields a surprisingly constant value for the plasma frequency  $\hbar\omega_p \approx 0.85$  eV over a wide range of  $x$  as shown in Fig. 4. By contrast, the oscillations of holes in an effective-mass approximation would yield  $\omega_p \propto x^{1/2}$  as denoted by the dotted curve.

Two-dimensional electronic oscillations in layered structures yield a spectrum of modes ranging from acoustic plasmons with vanishing plasmon frequency at long wavelengths to an optical branch which is produced by interlayer Coulomb coupling. Reflectivity should be dominated by the optical plasmon branch whose frequency  $\omega_p$  follows from

$$\hbar^2\omega_p^2 = \frac{4\pi e^2}{d\epsilon_\infty} \frac{2}{(2\pi)^2} \int d^2k \delta(E_k - E_F) [v_x(\mathbf{k})]^2, \quad (25)$$

where  $d$  is the spacing between Cu-O planes and  $\epsilon_\infty$  is the background dielectric constant. The combined contributions of the  $E_l$  and  $E_h$  bands give

$$\hbar^2\omega_p^2 = \frac{16e^2}{\pi d\epsilon_\infty} (t_l B_l + t_h B_h), \quad (26)$$

where the tight-binding functions are defined above, and  $d=13.7$  Å. A background dielectric constant of  $\epsilon_\infty \approx 8.4$  yields a relatively constant plasma frequency  $\hbar\omega_p \approx 0.85$  eV as shown in Fig. 4 for a wide range of Sr concentrations. The primary contribution to the plasmon response from the  $E_l$  band actually decreases slightly as added Sr concentrations lower the Fermi energy, but this decrease

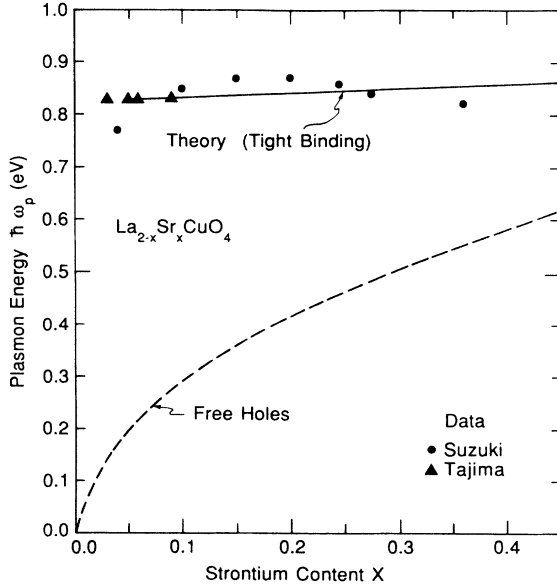


FIG. 4. Plasmon energy estimated from the reflectivity data of Suzuki (Ref. 3) and Tajima *et al.* (Ref. 14) on single-crystal film. The solid curve shows the optical plasmon energy calculated for the two-band model in the long-wavelength limit. The corresponding prediction of a single hole band in the effective-mass approximation, with  $m^* = m_e$ , is shown by the dashed curve.

is offset by the rise in the narrower  $E_h$  band contribution which is smaller in magnitude. The value of  $\epsilon_\infty$  was chosen to fit the experimental points corresponding to the observed dip in the reflectivity near 0.85 eV which are shown in Fig. 4. Had we chosen  $\epsilon_\infty = 1.0$ , the model would have  $\hbar\omega_p \approx 2.5$  eV which is not far from the value  $\hbar\omega_p \approx 2.9$  eV obtained in Ref. 6 from more sophisticated numerical computations and a different band structure.

## V. CONCLUSIONS

Any theory of the mechanism for high-temperature superconductivity is subject to the constraints imposed by Hall effect data particularly since the carrier concentration is such a vital ingredient. In the  $\text{La}_{2-x}\text{Sr}_x\text{CuO}_4$  case, the observed superconducting transition temperature rises sharply at  $x \approx 0.07$ , increases to  $T_c \approx 35$  K at  $x \sim 0.15$ , and then drops to zero in the regime  $x > 0.3$ . Thus the observed variation of  $T_c(x)$  would appear to have little direct connection with the  $R_H(x)$  behavior at first glance.

A superconductivity mechanism based on acoustic plasmons<sup>15</sup> emanating from two bands exhibits the physical ingredients which may be compatible with the  $T_c(x)$  variation as well as the detailed Hall data discussed here. The onset of superconductivity at small  $x \approx 0.07$  corresponds to a slight intersection of the Fermi energy  $E_F$  with the narrower  $E_h$  band which produces a very low energy acoustic plasmon with a typical cutoff energy  $\Theta_{pl}$ . Exchange of such plasmon modes yields a pairing in-

teraction for electrons in the wider  $E_l$  band and a BCS-like relationship  $T_c \propto \Theta_{pl}$  would account for the increase of  $T_c$  with Sr doping  $x$ . Then, as the Sr content becomes large, say  $x \geq 0.3$ , the plasmon exchange should fail to overcome the Coulomb repulsion between electrons whenever  $\Theta_{pl}$  exceeds a critical fraction of the Fermi energy.<sup>15</sup> Thus the observed<sup>16</sup> variation of  $T_c$  as a function of Sr content may be compatible in a qualitative sense with the electronic structure derived in the present analysis of the Hall effect and plasmon response.

Thermopower data<sup>17</sup> on ceramic  $\text{La}_{2-x}\text{Sr}_x\text{CuO}_4$  samples reveal a sign change at high temperatures which provide independent evidence for the presence of electrons and holes. Moreover, recent measurements<sup>18</sup> on a single crystal of  $\text{La}_{1.85}\text{Sr}_{0.15}\text{CuO}_4$  reveal a thermopower which is independent of magnetic field up to 30 T and is negative in the Cu-O plane direction in sharp contrast to a hopping model for a strongly Coulomb correlated system. Although the observed negative thermopower supports the presence of electrons in accord with the structure proposed in the present paper, a detailed study of the thermopower is required to test the quantitative validity of our theory.

The symmetry properties of the two bands do not enter our calculations in a specific way, although the two-dimensional structure and the likely Cu  $d_{x^2-y^2}$  origin of the  $E_l$  band are compatible with the band structure results. The origin of the second band ( $E_h$ ) close to the Fermi energy may be the Cu  $d_{z^2}$  level hybridized with the oxygen  $p$  state. However, other candidates for the narrow  $E_h$  band are not excluded by our analysis, and other cuprate alloys may perhaps yield the coexistence of a nearly half-filled energy band with another narrower partially filled state.

The sensitivity of our results for the electron-electron scattering cross section to the logarithmic density of states in the 2D tight-binding model is open to criticism. The present Hall effect calculation suggests that the electron mobility is an extremely sensitive function of Sr content, and it is worthwhile to consider other explanations for this surprising feature. An effective-mass approximation would yield a constant 2D density of states with very little dependence of the electron-electron cross section on the doping for  $x > 0.1$ . Another possibility is the more general feature of a "nested" Fermi surface with nearly parallel curvature over some momentum region  $\mathbf{q} \approx \mathbf{Q}$  such that  $\epsilon(\mathbf{k}) + \epsilon(\mathbf{k} + \mathbf{Q}) \approx 0$ : In the nested Fermi liquid (NFL) the susceptibility and therefore the electron-electron scattering cross section is strongly influenced by shifts in the Fermi energy. The multiple-scattering processes in that case<sup>19</sup> resemble the present results for the electron mobility even though the NFL analysis approximates the density of states by a constant  $N(E_F)$  and considers the primary influence of nesting on the susceptibility. It would be interesting to examine other Fermi surface "nesting" models in addition to the 2D tight-binding bands considered here.

Our estimate for the Coulomb coupling  $U$  is crude at best. Given our reliance on a highly idealized 2D tight-binding band which shows a logarithmic singularity in

the density of states, we obtain a reasonable fit with  $U \approx 0.7$  eV in comparison to the bandwidth  $W = 4.0$  eV. Topological distortions of the  $E_f$  band are in fact evident in the band structure calculations, and the associated reduced Fermi surface nesting should diminish  $\chi'(\mathbf{Q}, E_F)$  and thereby elevate the value of  $U$  needed to achieve a fit to the Hall data. Nevertheless, the itinerant nature of the electronic states seems to be compatible with the main features of the measured Hall coefficient and resistivity.

Another consequence of nesting is the possible formation of pseudogaps in the spectrum<sup>20</sup> which have been investigated in connection with the spin-bag mechanism for high- $T_c$  superconductivity. The latter work reports numerical results for the Hubbard model which show structure in the density of states that should also be susceptible to shifts in the Fermi energy.

Finally, we remark on the implications of our findings for the electronic response at finite frequencies. The static limit for the electron cross section gives<sup>9</sup>  $\tau_l^{-1}(\omega=0, x=0) \propto T$ , where on-site Coulomb coupling  $U$  dominates the scattering for perfect nesting of the exactly half-filled tight-binding band. More generally, the elec-

tron lifetime for a partially nested Fermi surface is<sup>19</sup>  $\tau_l^{-1}(\omega=0, x) = \alpha T$ , where  $\alpha$  is a measure of  $U$  relative to the bandwidth, and the variation of  $\alpha(x)$  with the extent of nesting is determined by the Sr content. For finite frequencies  $\omega > T$ , the corresponding result is<sup>19</sup>  $\tau_l^{-1}(\omega > T) \approx \alpha \omega$  and this frequency variation is substantial for intermediate coupling  $0.5 < \alpha < 1$ . A confirmation of such an unconventional frequency dependence has just been discovered in photoemission spectra of  $\text{Bi}_2\text{Sr}_2\text{CaCu}_2\text{O}_8$  with  $\alpha \approx 0.7$ .<sup>21</sup> The corresponding frequency variation will affect the Drude relaxation rate which is used in the analysis of the infrared reflectivity. Thus the shape of the reflectivity curve and the plasma frequency required to achieve a fit will also be affected by these electron scattering processes.

#### ACKNOWLEDGMENTS

It is a pleasure to acknowledge stimulating comments by A. K. Rajagopal, J. R. Schrieffer, and A. Zawadowski. This research is supported by the U.S. Department of Energy Grant No. DEF 605-84-ER 45113.

\*Permanent address: Central Research Institute for Physics, H-1525 Budapest 114, P.O. Box 49, Hungary.

<sup>1</sup>J. G. Bednorz and K. A. Müller, Z. Phys. B **64**, 189 (1986).

<sup>2</sup>N. P. Ong, Z. Z. Wang, J. Clayhold, J. M. Tarascon, L. H. Greene, and W. R. McKinnon, Phys. Rev. B **35**, 8807 (1987).

<sup>3</sup>M. Suzuki, Phys. Rev. B **39**, 2312 (1989).

<sup>4</sup>L. F. Mattheiss, Phys. Rev. Lett. **58**, 1028 (1987).

<sup>5</sup>J. Yu, A. J. Freeman, and J. H. Xu, Phys. Rev. Lett. **58**, 1035 (1987).

<sup>6</sup>P. B. Allen, W. E. Pickett, and H. Krakauer, Phys. Rev. B **36**, 3926 (1987).

<sup>7</sup>J. E. Hirsch and D. J. Scalapino, Phys. Rev. Lett. **56**, 2732 (1986).

<sup>8</sup>Y. Hasegawa and H. Fukuyama, Jpn. J. Appl. Phys. **26**, L322 (1987).

<sup>9</sup>P. A. Lee and N. Read, Phys. Rev. Lett. **58**, 1691 (1987).

<sup>10</sup>I. E. Dzyaloshinski, Zh. Eksp. Teor. Fiz. **93**, 1487 (1987) [Sov. Phys.—JETP **66**, 848 (1987)].

<sup>11</sup>H. Takagi, T. Ido, S. Ishibashi, M. Uota, S. Uchida, and Y. Tokura, Phys. Rev. B **40**, 2254 (1989).

<sup>12</sup>C. W. Chu, P. H. Hor, R. L. Meng, L. Gao, Z. J. Huang, and Y. Q. Wang, Phys. Rev. Lett. **58**, 405 (1987).

<sup>13</sup>N. W. Preyer, R. J. Birgeneau, C. Y. Chen, D. R. Gabbie, H. P. Jenssen, M. A. Kastner, P. J. Picone, and T. Thio, Phys. Rev. Lett. **63**, 2307 (1989).

<sup>14</sup>S. Tajima, S. Uchida, S. Tanaka, S. Kanbe, K. Kitazawa, and K. Fueki, Jpn. J. Appl. Phys. **26**, L432 (1987).

<sup>15</sup>J. Ruvalds, Phys. Rev. B **35**, 8869 (1987).

<sup>16</sup>J. B. Torrance, Y. Tokura, A. I. Nazzari, A. Bezing, T. C. Huang, and S. S. P. Parkin, Phys. Rev. Lett. **61**, 1127 (1988).

<sup>17</sup>C. Uher, A. B. Kaiser, E. Gmelin, and L. Walz, Phys. Rev. B **36**, 5676 (1987).

<sup>18</sup>R. C. Yu, M. J. Naughton, X. Yan, P. M. Chaikin, F. Holtzberg, R. L. Greene, J. Stuart, and P. Davies, Phys. Rev. B **37**, 7963 (1988).

<sup>19</sup>A. Virosztek and J. Ruvalds (unpublished).

<sup>20</sup>A. Kampf and J. R. Schrieffer, Phys. Rev. B **41**, 6399 (1990).

<sup>21</sup>C. G. Olson, R. Liu, D. W. Lynch, R. S. List, A. J. Arko, B. W. Veal, Y. C. Chang, P. Z. Jiang, and A. P. Paulikas, Phys. Rev. B **42**, 381 (1990).